Supporting Information for

Transient DNA Damage Following Exposure to Gold Nanoparticles

Sarah May,[ab] Cordula Hirsch,[a] Alexandra Rippl,[a] Nils Bohmer,[a†] Jean-Pierre Kaiser,[a] Liliane Diener,[a] Adrian Wichser,[a] Alexander Bürkle[b] and Peter Wick[a]*

[a.] *Particles-Biology Interactions Laboratory, Swiss Federal Laboratories for Materials Science and Technology (Empa), Lerchenfeldstrasse 5, CH-9014, St. Gallen, Switzerland*

[b.] *University of Konstanz, Molecular Toxicology Group, Universitätsstrasse 10, D-78464 Konstanz, Germany*

† Current address: DECHEMA e.V., Research Management and Conferences, Theodor-Heuss-Allee 25, 60486 Frankfurt am Main, Germany

Corresponding author

Email: peter.wick@empa.ch

ORCID: Peter Wick: 0000_0002_0079_4344

TEM

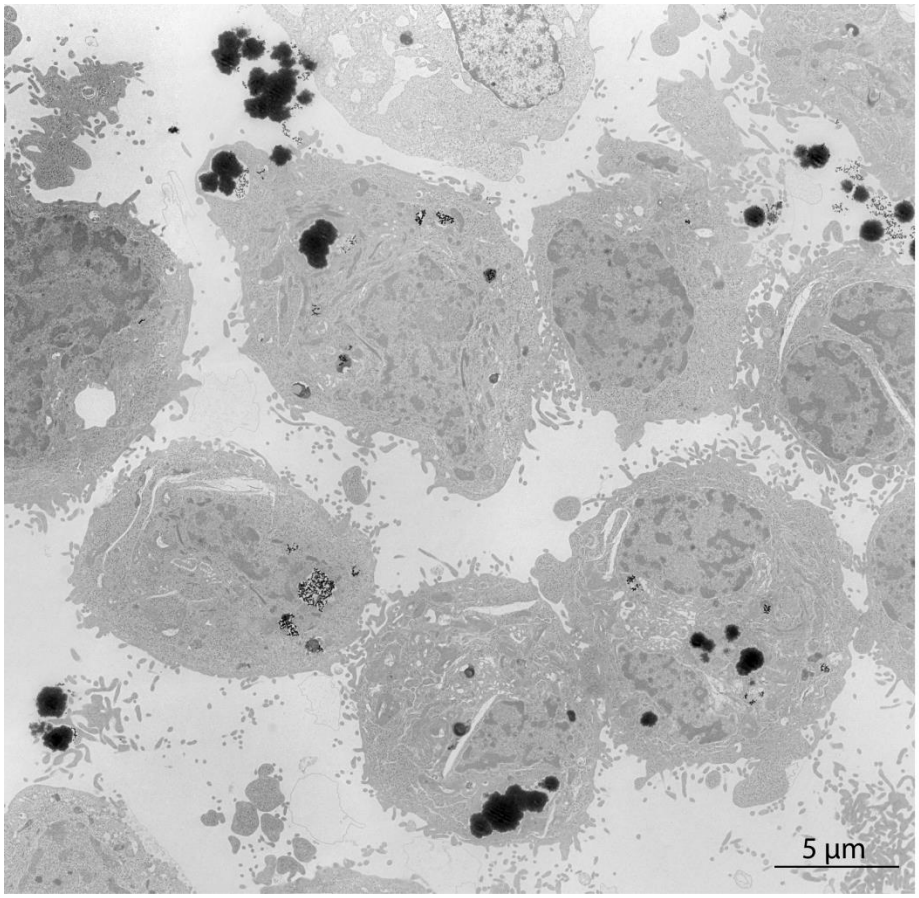

Figure S1. TEM micrograph showing the presence of agglomerated Au-NP III inside and outside of A549 cells after 24 h exposure to 100 µg/ml. An overview of differently sized and shaped structures is shown.

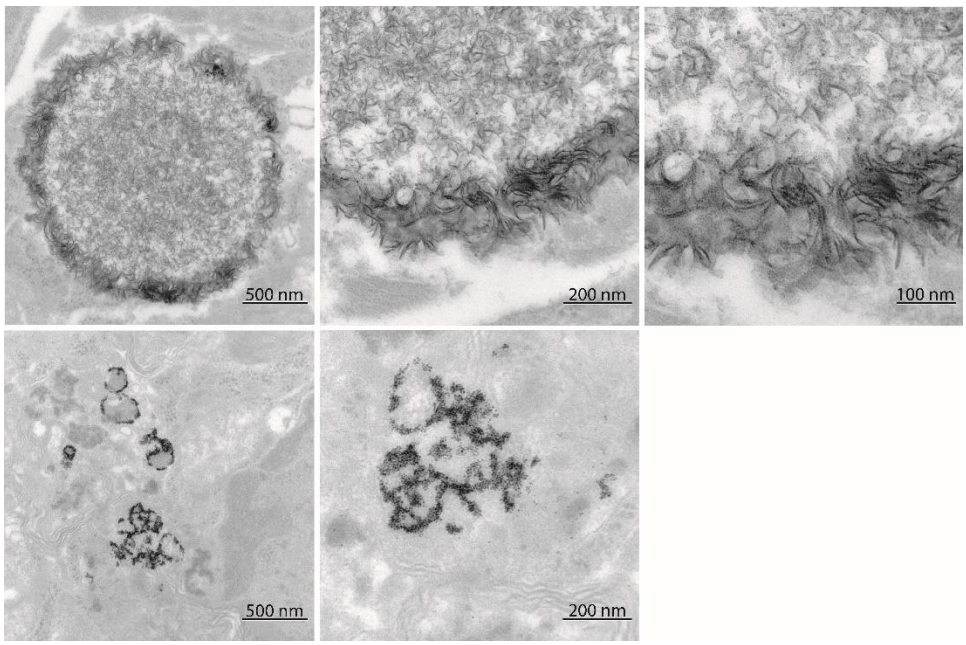

Figure S2. TEM micrograph showing the magnifications of differently structured Au-NP agglomerates in A549 cells after 24 h exposure to 100 µg/ml Au-NP III.

H_2-DCF assay in THP-1 cells

As opposed to A549 cells, THP-1 monocytes were seeded into 96-well plates at a density of $8x10^4$ cells per well in a total volume of 200 µl complete cell culture medium containing 200 nM PMA. Cells were allowed to differentiate for 72 h in the presence of PMA and were washed twice with 200 µl pre-warmed PBS prior to treatment. Thereafter, intracellular reactive oxygen species (ROS) were detected using 2', 7'-dichlorofluorescin diacetate (H_2-DCF-DA) according to the protocol described in materials and methods. Data shown represent the mean and corresponding standard deviation of three independent experiments with three technical replicates each.

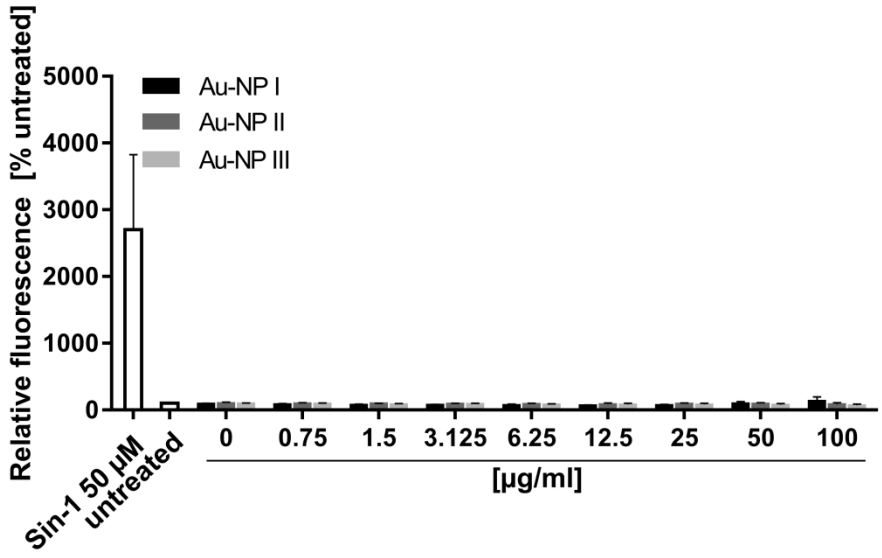

Figure S3. Au-NPs do not induce ROS generation in THP-1 cells. Data shown represent the mean of three independent experiments and the corresponding standard deviations of the 3 h reading point.

Interference assessment in a cell-free environment

Diverse types of nanomaterials have been shown to interfere with different fluorimetric as well as colorimetric *in vitro* assays[1-6] (for a review see Kroll et al., 2009[7]). To avoid false positive as well as false negative results it is therefore very important to address potential interferences prior to or in parallel with the actual cellular experiments. We have established cell free interference controls for different assays that are run independently of the cell based assays.

Interference assessment in the H_2-DCF assay

Three parameters of potential Au-NP interference with the H_2-DCF assay were assessed in a cell free setup: autofluorescence, quenching of an existing fluorescence signal by Au-NP and oxidation of H_2-DCF due to intrinsic Au-NP (surface) reactivity. The treatment of interference control samples and the assay procedure were identical to the protocol described in materials and methods. Data shown represent the mean and corresponding standard deviation of at least two independent experiments with three technical replicates each.

To assess auto-fluorescence of Au-NPs 50 µL of increasing Au-NP concentrations diluted in HBSS buffer were incubated with 50 µl ddH_2O under the same culture conditions as for cellular experiments. Figure S5a shows the 3 h reading point in the cell free interference control assay. Fluorescence was always measured using a plate reader (Mithras^2, Berthold Technologies). None of the three Au-NPs shows auto-fluorescence at an excitation wavelength of 485 nm and an emission wavelength of 528 nm at all concentrations and time points investigated.

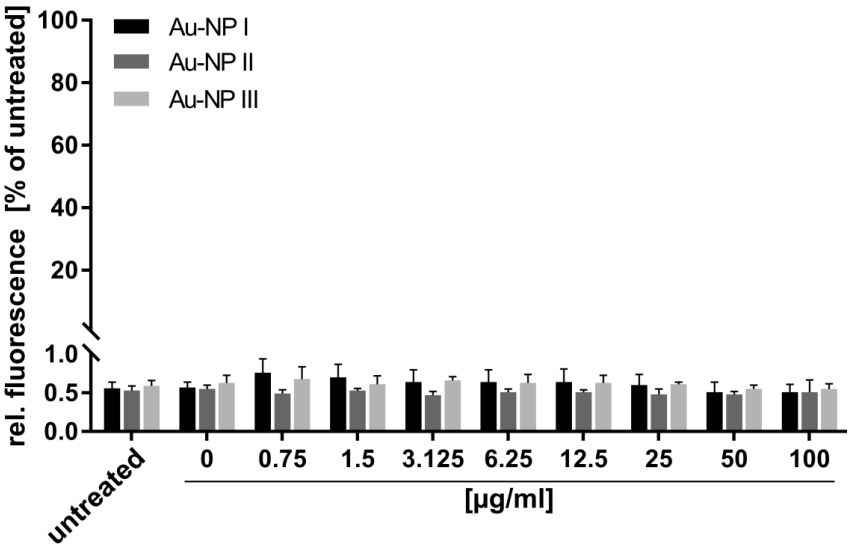

Figure S8a. Au-NP are not autofluorescent. Data shown represent the mean of three independent experiments and the corresponding standard deviations.

To determine the influence of Au-NP induced quenching on an existing fluorescence signal, the fluorescent dye DCF (Sigma, Buchs, Switzerland) was added to a 96-well plate in a volume of 50 µL and a concentration of a 2.5 µM. 50 µL of increasing Au-NP concentrations diluted in HBSS were applied and fluorescence intensities were measured at an excitation wavelength of 485 nm and an emission wavelength of 528 nm. Figure S5b shows the 3 h reading point in the cell free interference control assay. All three Au-NP types reduce the existing DCF signal in a dose-dependent manner. At the highest concentration of 100 µg/ml Au-NP the remaining signal is approximately 60% of the initial value for all particles. The

quenching effect is least prominent for neutral Au-NPs. The observed effects are rather small, but they still need to be taken into account when interpreting cellular responses.

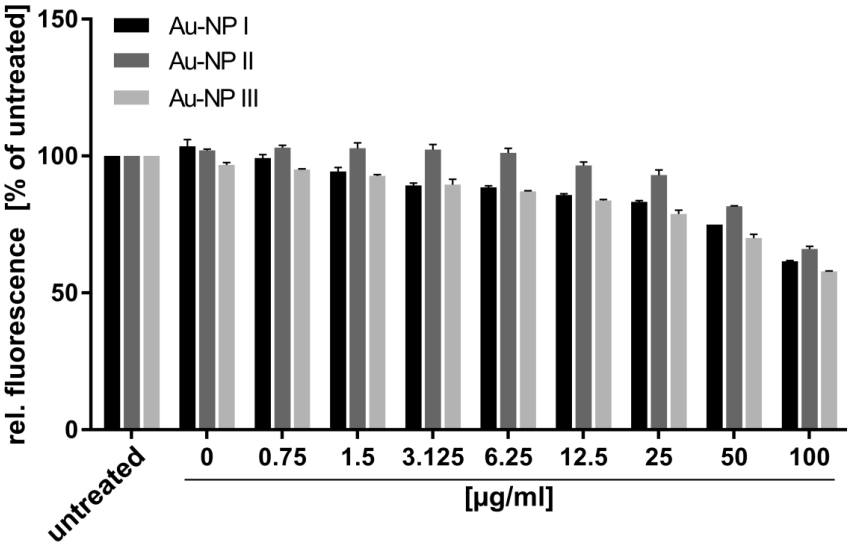

Figure S8b. Au-NP quench an existing DCF signal slightly in a dose-dependent manner. The weakest effect is caused by Au-NP II. Data shown represent the mean of two independent experiments and the corresponding standard deviations.

To assess the intrinsic activity of Au-NPs to process the H_2-DCF molecule to its fluorescent form (DCF), the H_2-DCF-DA has to be deacetylated prior to incubation with Au-NPs. Therefore, 0.5 ml 5 mM H_2-DCF-DA was added to 2.5 ml Methanol and 10 ml 0.01 M NaOH and stirred for 30 minutes at room temperature (RT) in the dark. The reaction was stopped by adding 37.5 ml 33 mM NaH_2PO_4. 50 µl of deacetylated ROS sensitive H_2-DCF molecule was incubated with 50 µl increasing concentrations of Au-NPs diluted in HBSS. Fluorescence intensities were measured at an excitation wavelength of 485 nm and an emission wavelength of 528 nm. The intensity of DCF fluorescence is indicative of the intrinsic reactivity of the substance/particle under investigation. As depicted in Figure S8c the chemical positive control Sin-1 leads to a ~55-fold increase in relative fluorescence values compared to the untreated sample. Au-NP I increases fluorescence dose-dependently up to 6-fold at 100 µg/ml. This effect, compared to the positive control, is rather small. Nevertheless, values measured in the presence of cells might not be solemnly due to cellular reactions but a combination of intrinsic particle reactivity and cellular responses. In contrast Au-NP II and III did not oxidize H_2-DCF to its fluorescent form DCF. This indicates no intrinsic reactivity of those nanoparticles towards H_2DCF.

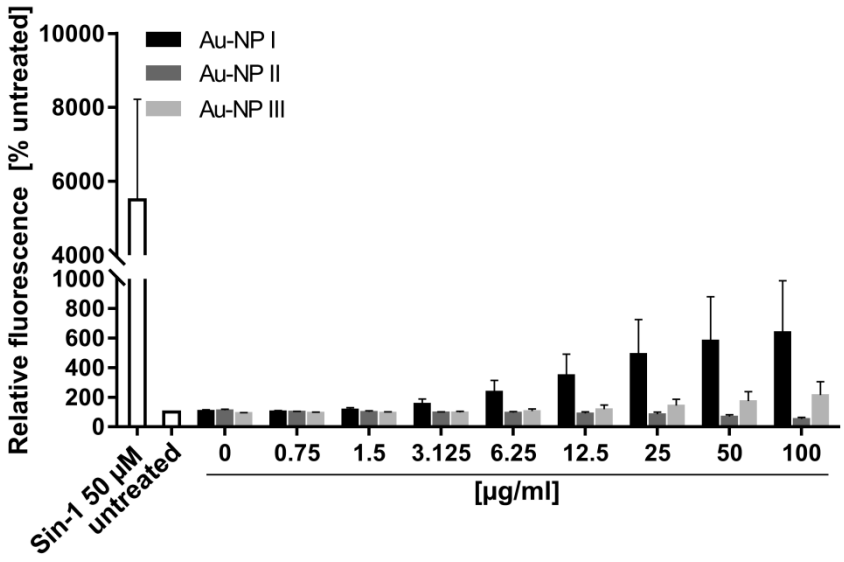

Figure S8c. Au-NP I process H_2-DCF in a cell free setup whereas Au-NP II and Au-NP III do not. Sin-1 served as chemical positive control and increases fluorescence after 3 h of incubation. Data shown represent the mean of two independent experiments and the corresponding standard deviation.

Interference assessment in the MTS assay

Three parameters of potential Au-NP interference with the MTS assay were assessed: intrinsic absorbance signal of Au-NPs, the ability of Au-NPs to reduce MTS without cellular contribution and the influence of Au-NPs on absorbance values of the reduced MTS (formazan). The treatment of interference control samples and the assay procedure were identical to the protocol described in materials and methods. Data shown represent the mean and corresponding standard deviation of three independent experiments with two technical replicates each.

For assessment of a potential intrinsic absorbance signal of Au-NPs within the MTS assay 100 µl of increasing Au-NP concentrations are incubated under the same culture conditions as in the cellular experiments with 100 µl phenolred-free RPMI media. To determine the potential Au-NP-dependent reduction of MTS in a cell-free system 5 ml RPMI without phenol red were mixed with 1 ml MTS (stock). 100 µl thereof were mixed with 100 µl of Au-NP concentrations. To determine the influence of Au-NPs on reduced MTS, 5 ml RPMI without phenol red were mixed with 1 ml MTS and 50 µl 100 mM Na_2SO_3. 100 µl of reduced MTS was incubated with different concentrations of Au-NPs in a volume of 100 µl. After 1 h of incubation absorbance at 490 nm was measured in a plate reader (Mithras^2, Berthold Technologies).

As shown in Figure S4 a-c all three types of Au-NPs increase absorbance values (λ=490 nm) at concentrations above 25 µg/ml. Slopes measured in phenolred-free RPMI (white rhombs "blanks"), in MTS (grey squares) and in formazan (black circles) are the same. This indicates that bare Au-NPs ("blanks") show a certain intrinsic absorbance but are not reactive, i.e. do not process MTS or formazan. Blank values can therefore be subtracted from values measured in MTS and formazan. The resulting blank-corrected values are shown in Figure S4 a'-c'. The dotted line in these plots indicates the absorbance value of formazan (no Au-NP added) measured at 490 nm after blank subtraction. Subtracting blank values at corresponding Au-NP concentrations corrects for the increase of absorbance at Au-NP concentrations above 25 µg/ml. These results justify the approach of subtracting blank values that are measured side by side with every cell-based assay.[8]

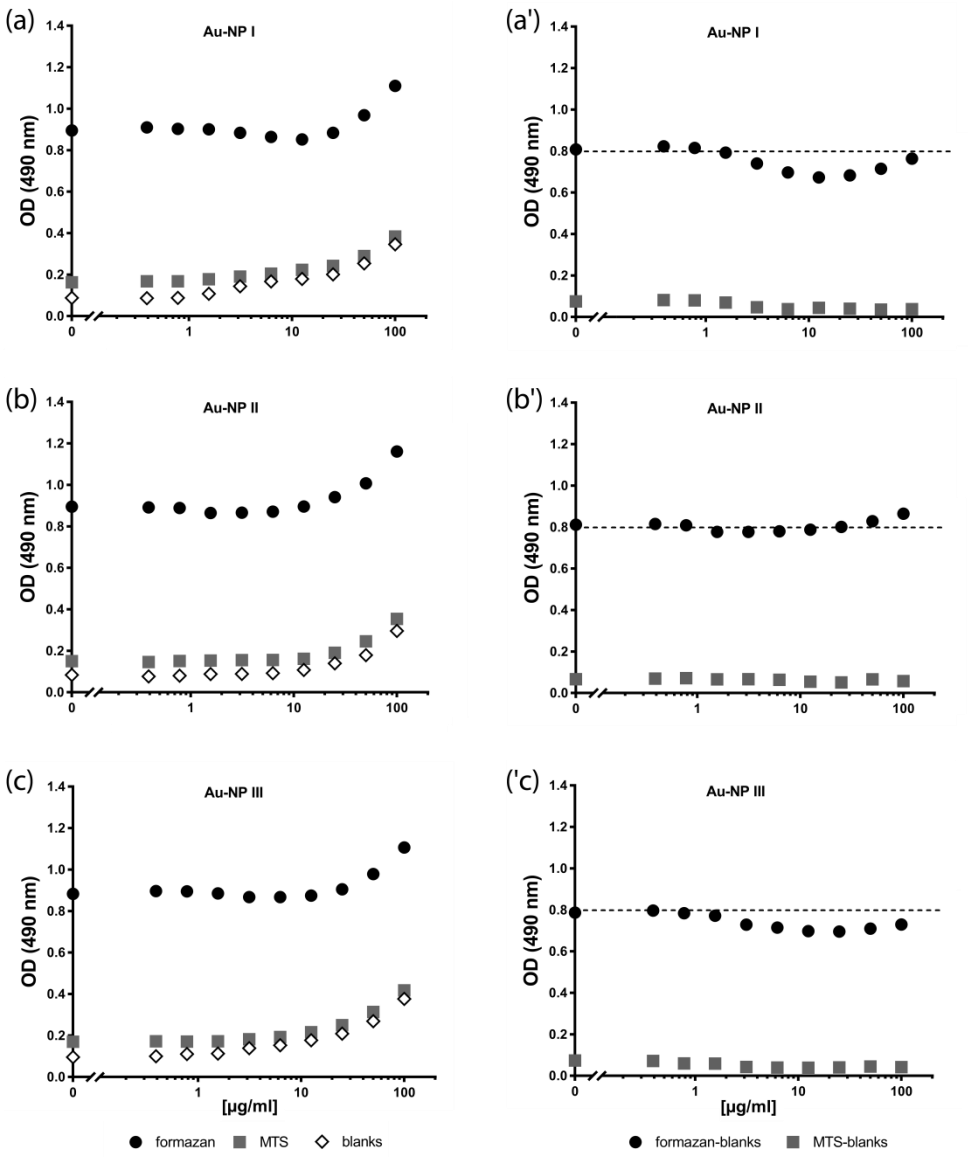

Figure S4. Au-NP interference with the MTS assay is assessed regarding intrinsic absorbance signal of Au-NPs (white rhombs "blanks"), the ability of Au-NPs to reduce MTS (grey squares) and the influence of Au-NPs on absorbance values of the reduced MTS (black circles). All Au-NPs increase absorbance at 490 nm (white rhombs "blanks") indicating intrinsic absorbance, but do not process the MTS reagent (grey squares) or influence the formazan product (black dots) as all three slopes are very similar (a) Au-NP I, (b) Au-NP II, (c) Au-NP III. (a', b', c') Blank corrected absorbance values. Dotted line depicts the OD_{490nm} value of formazan after blank subtraction (without addition of Au-NPs). Data shown represent the mean of three independent experiments.

Interference assessment in the LDH assay

In order to assess potential NP interferences with the LDH assay four different parameters were investigated: generation of intrinsic absorbance signal of Au-NPs and its behavior over time (in KPP buffer only), potential NP interaction with pyruvate that might affect measurements over time (KPP buffer + pyruvate), potential NP interaction with NADH that might affect measurements over time (KPP buffer + NADH), and potential NP interference on the combined components (KPP buffer + Pyruvate and NADH). The treatment of interference control samples and the assay procedure were identical to the protocol described in materials and methods. Data shown represent the mean of three independent experiments with two technical replicates each.

Increasing concentrations of Au-NPs were diluted in 100 µl RPMI medium and to mimic what happens during cell lysis, NPs were diluted in lysis buffer as well and processed according to the cell lysis protocol (see Materials and Methods). 20 µl of each NP dilution in medium and lysis buffer were transferred to a 96-well plate. For the enzymatic reaction, 180 µl of the different reaction buffer either containing only KPP, KPP and sodium pyruvate (240 µM), KPP and NADH (616 µM) or all components combined, were added. The absorption was measured using a multi-well plate reader (Mithras^2, Berthold Technologies) at 360 nm at 37°C in 1 min intervals over a time period of 15 min.

None of the three Au-NPs, whether incubated in media or in lysis buffer, revealed any interference with the LDH assay (Figure S5 a-d, a'-d'). Over the duration of the measurement there was no significant increase of absorption values independent of the respective buffer (KPP buffer only, KPP buffer + pyruvate, KPP buffer + NADH, KPP buffer + Pyruvate and NADH).

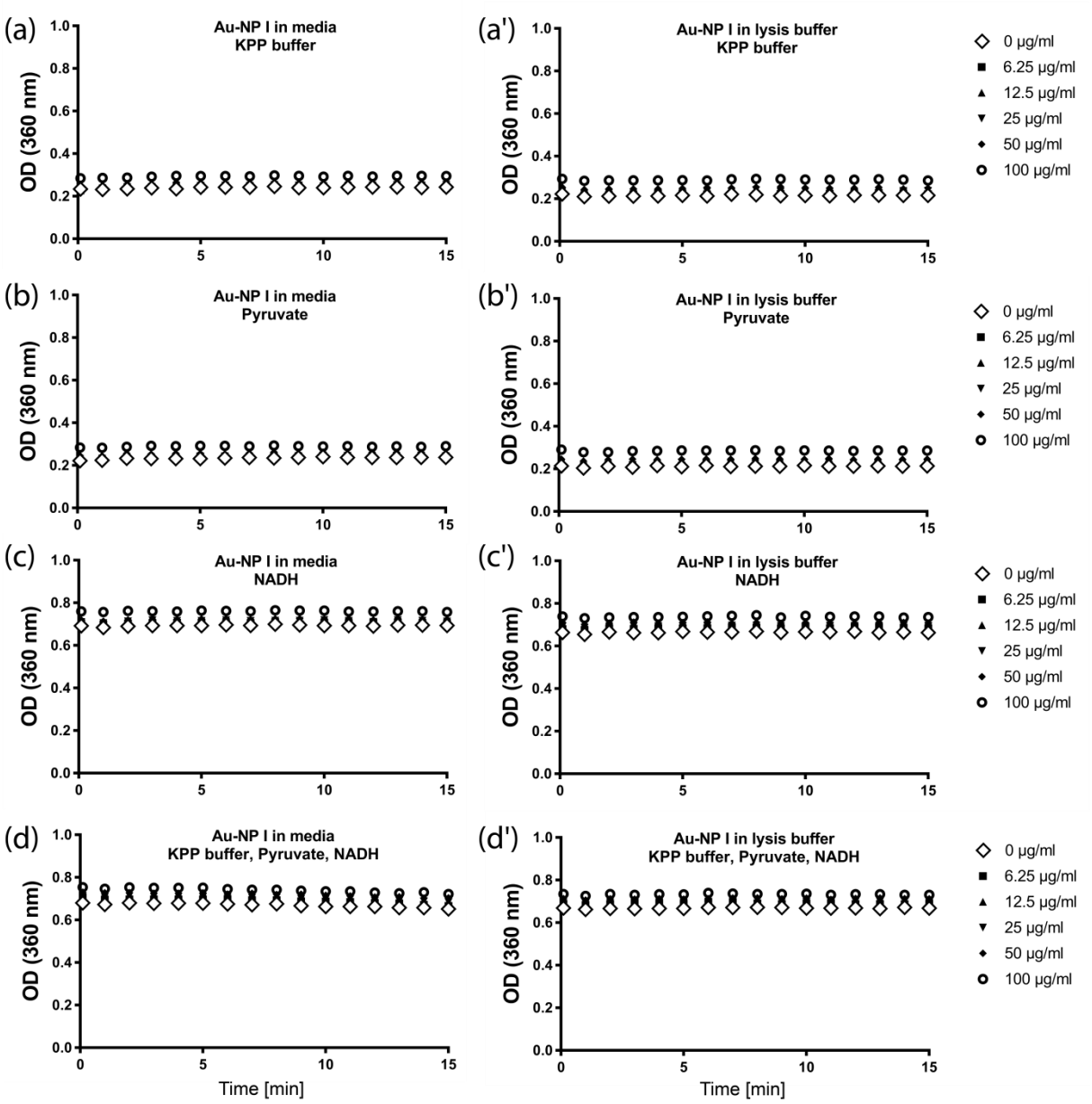

Figure S5. Au-NP I show no interference with the LDH assay. There is no influence of nanoparticles on absorbance at 360 nm in medium (a, b, c, d) or in lysis buffer (a‘, b‘, c‘, d‘) over a time period of 15 minutes. Also the different assay components, such as KPP buffer (a, a‘), pyruvate (b, b‘), NADH (c, c‘) and all components combined (d, d‘) reveal no significant influence on absorption values. Data shown represent the mean of three independent experiments.

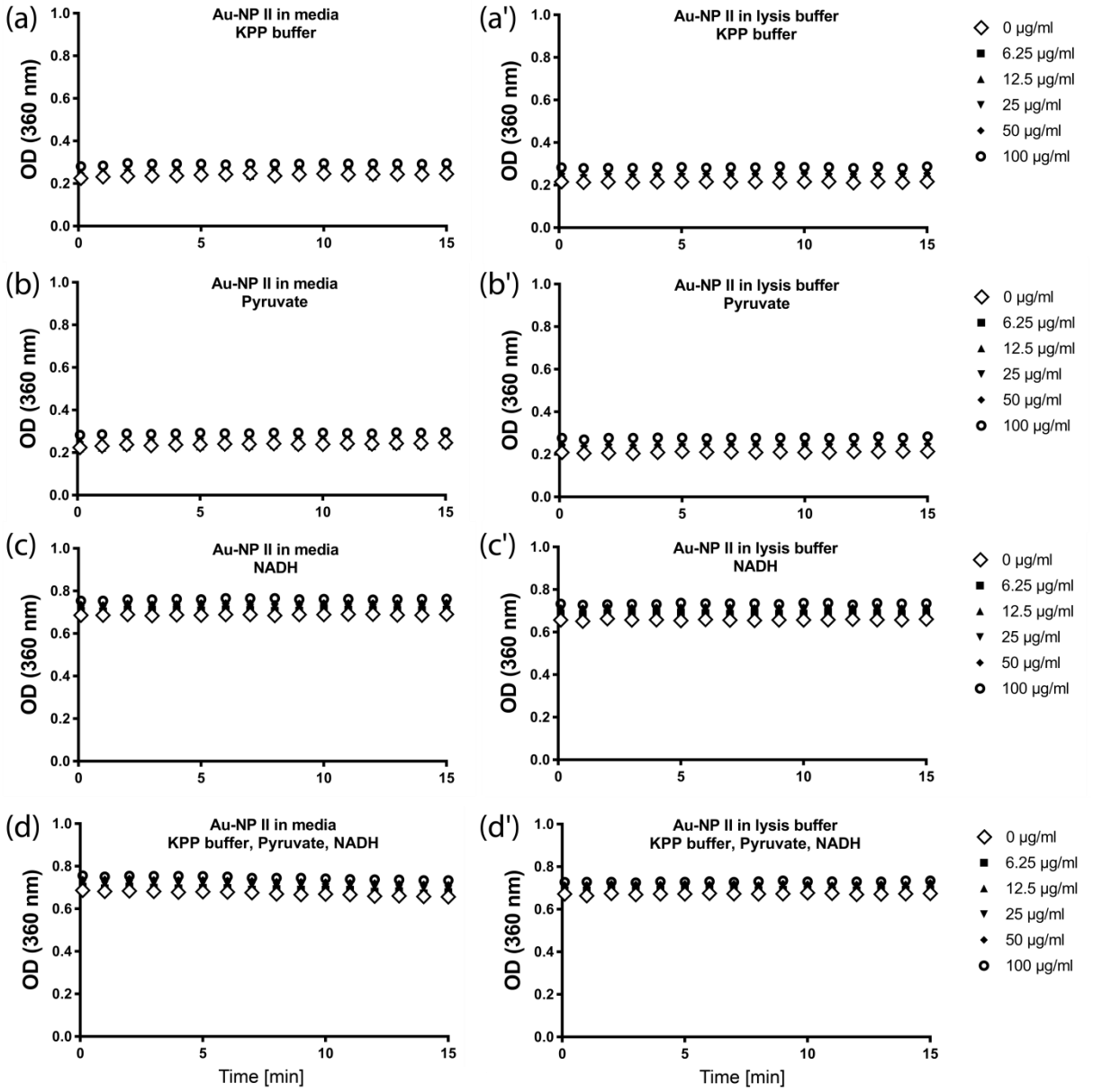

Figure S6. Au-NP II show no interference with the LDH assay. There is no influence of nanoparticles on absorbance at 360 nm in medium (a, b, c, d) or in lysis buffer (a‘, b‘, c‘, d‘) over a time period of 15 minutes. Also the different assay components, such as KPP buffer (a, a‘), pyruvate (b, b‘), NADH (c, c‘) and all components combined (d, d‘) reveal no significant influence on absorption values. Data shown represent the mean of three independent experiments.

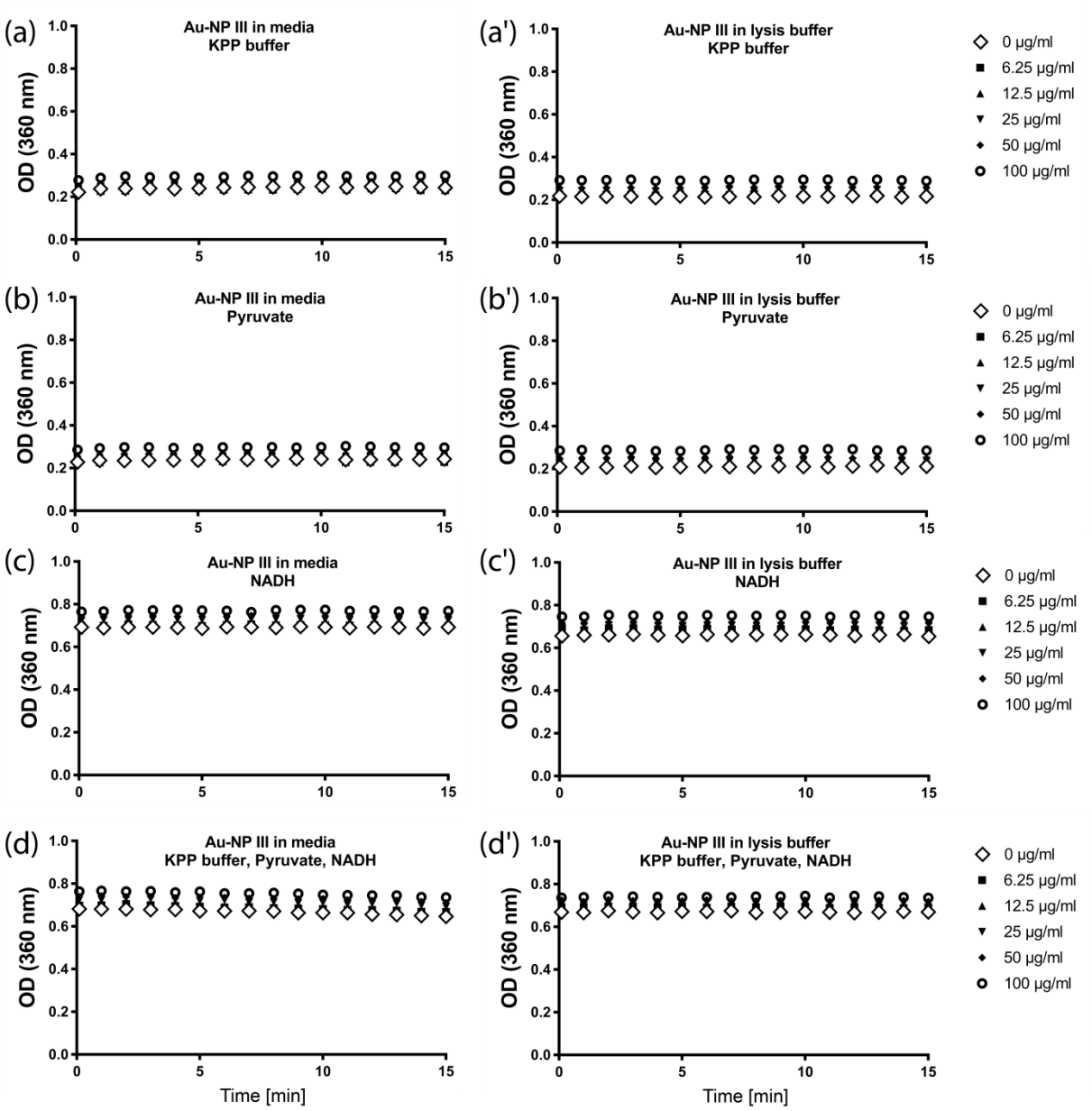

Figure S7. Au-NP III show no interference with the LDH assay. There is no influence of nanoparticles on absorbance at 360 nm in medium (a, b, c, d) or in lysis buffer (a‘, b‘, c‘, d‘) over a time period of 15 minutes. Also the different assay components, such as KPP buffer (a, a‘), pyruvate (b, b‘), NADH (c, c‘) and all components combined (d, d‘) reveal no significant influence on absorption values. Data shown represent the mean of three independent experiments.

Interference assessment in the GSH assay

Two parameters of potential Au-NP interference with the GSH assay were determined in a cell free setup: interference of Au-NP in solution containing all assay relevant components (MPA/MES/TEAM) and the influence of Au-NPs on the GSSG standard (8 µM). Here, the following concentration range of Au-NPs was used: 80, 40, 20, 10, 5, 2.5, 1.25 µg/ml. Each concentration was prepared in the 8 µM GSSG standard or in a solution of MES buffer, MPA and TEAM in the exact dilution as used for the cellular assay. 50 µl of each sample, as well as the GSSG standard were transferred to a 96-well plate and 150 µl of the freshly prepared assay cocktail was applied to each well. After 25 min incubation in the dark absorbance was measured at 405 nm wavelength in a multi-well plate reader (Mithras^2, Berthold Technologies). Data shown represent the mean of at least three independent experiments.

All three Au-NPs, when incubated in the assay solution showed slightly enhanced absorbance values for the highest concentration of 80 µg/ml (black squares, Figure S9). This concentration was used as worst case scenario since it is certainly much higher than the actual concentration in the cellular GSH assay. For collection of those samples the supernatant containing remaining Au-NPs is removed, cells are washed and two centrifugation steps are performed. After these only the supernatant is used for the following procedure and therefore the concentration was expected to be quite low. This was confirmed by ICP-MS measurements which revealed an Au concentration of 1.08 µg/ml in the processed cell lysate (mean of two independent measurements with duplicates each). Of the cell lysate 50 µl were used in the cellular GSH assay. This is important to know when interpreting the interference results of Au-NPs diluted in the GSSG standard. Compared to the control absorbance values declined strongly in a dose-dependent manner for each type of Au-NP starting already at 1.25 µg/ml (white rhombs, Figure S9). However, the reduction in OD for this concentration is rather small and since the Au-NP concentration in the processed cell lysate is similarly low, the observed minor interferences for the relevant concentrations are negligible.

ICP-MS Analysis

Conventional ICP-MS analysis was performed in order to quantify Au-NP. Digestion of samples were performed in closed vials using 0.6 ml 67 % HNO3 and 1.8 ml 30 % HCl with the following temperature program. Total amount of Au in the samples was determined by Sectorfield ICP mass spectrometer SF-ICP-MS (Series 2, Thermo Fisher Scientific GmbH, Germany). The ICP-MS parameters were optimized. For the Au detection, the ^{197}Au isotope was selected. As an internal standard ^{40}Ar^{40}Ar and ^{187}Re were used. Prior to analysis, digested samples were filled up with ultrapure water to 10 ml with 10 ppb of ^{187}Re as internal standard. Calibrations were performed using an ionic Au standard in a matrix matched solution (0.6 ml of 67 % HNO3 and 1.8 ml of 30 % HCl per 50 ml) ranging from 0 to 50 µg/l Au.

Parameter/ICP-MS type	Thermo Fisher Scientific SF-ICP-MS
Plasma power	1200 W
Plasma gas flow rate	15 L/min
Carrier gas flow rate	0.8 L/min
Sample gas flow rate	0.784 L/min
Sample uptake flow rate	0.75 mLmin
Isotopes monitored	^{197}Au
Integration time per isotope	150 ms
Nebulizer type	MicroMist
Spray chamber type	Twister cyclonical Spray Chamber with Helix

Table 1: Program for tissue digestion with microwave system

Stage	**Time**	**T1(°C) inside**	**T2 (°C) outside**	**Presure (bar)**	**Power (W)**
1	2	80	60	100	1000
2	10	250	60	120	1000
3	8	250	60	120	1200

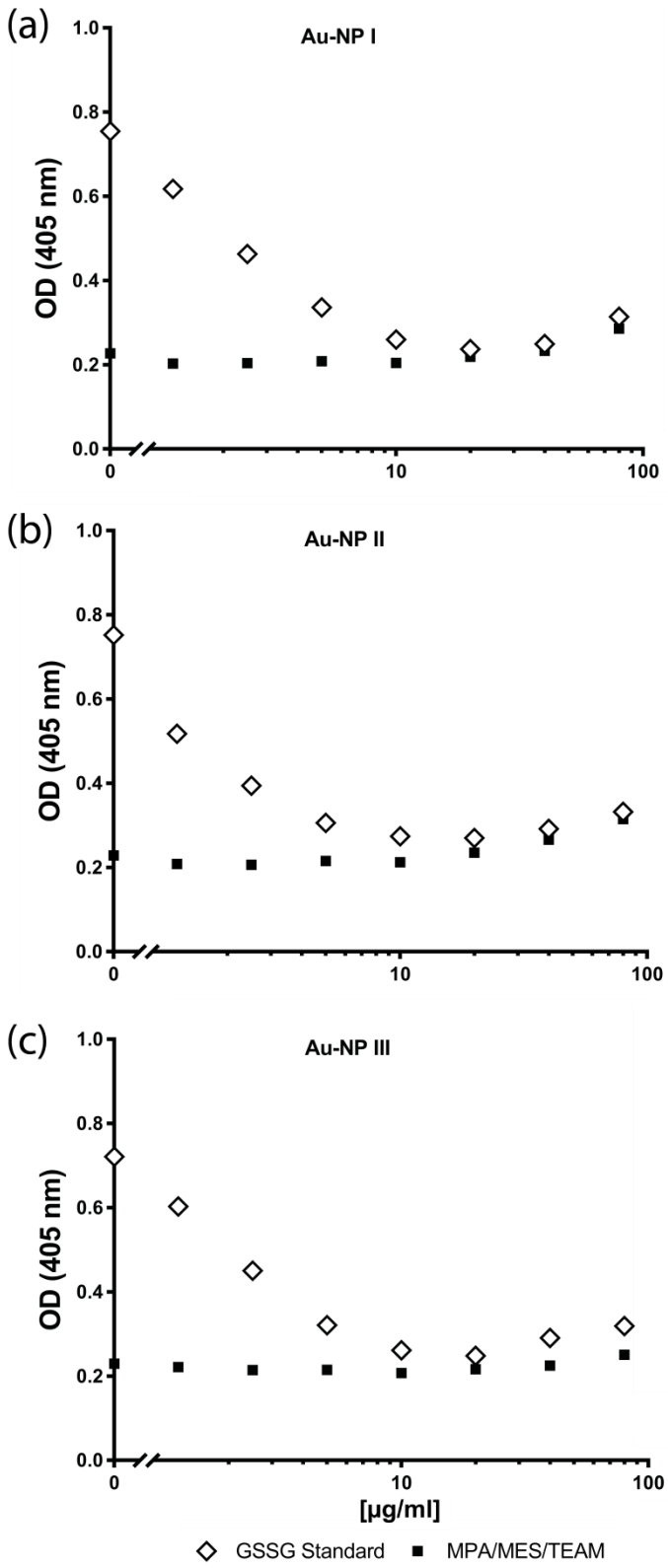

Figure S9. Au-NP interference with the GSH assay. Absorbance values of all three Au-NPs (a, b, c) diluted in MPA/MES/TEAM (black squares) increase slightly. Compared to the control the absorbance values of the GSSG standard at a concentration of 8 µM decrease already at the lowest concentration for all three Au-NPs (white rhombs). Data shown represent the mean of three independent experiments.

Interference assessment in cytokine release detection by ELISA (TNF-α)

As Au-NP interference could theoretically occur during all steps of an ELISA assay, four different parameters were assessed in a cell free setup: intrinsic catalytic activity in the presence and absence of the antigen, influence on optical density, Au-NP binding capability to antibodies (generating false positive results) and binding capability to the antigen itself (generating false positive or negative results). Detailed protocols for the cellular assay as well as the cell free interference assay can be found on the $DaNa^{2.0}$ homepage (www.nanopartikel.info).[9] The treatment of interference control samples and the assay procedure were identical to the protocol described in materials and methods. For assessment of potential Au-NP interference within the ELISA assay 100 µl of increasing Au-NP concentrations were used for each for the different setups. Data shown represent the mean of one to two experiments with two technical replicates each.

The potential intrinsic catalytic activity of Au-NPs was assessed in the presence (see Figure S10: 500 pg/ml standard (NP + substrate)) and absence of the antigen TNF-α (see Figure S10: Normal (NP + substrate). For this approach Au-NPs were spiked into the very last step of the ELISA procedure, i.e. together with the substrate. OD values for interference assessment without addition of the antigen were expected to be very low, whereas samples that were exposed to the antigen were expected to produce OD values of 1 or higher. Assessment of the intrinsic activity of Au-NPs in the absence of the antigen resulted in low OD values with a slight increase for the highest concentration of 100 µg/ml. This was observed for all the types of Au-NPs. In the presence of the antigen the OD values were higher as expected and the OD increased for all three Au-NPs starting at a concentration of 50 µg/ml. These results indicate a certain intrinsic catalytic activity of these particles at higher concentrations in the presence and absence of the antigen.

To determine the potential influence on the optical density Au-NPs were spiked in the assay diluent in the final step of the assay (see Figure 10S: Normal (NP + 1x assay diluent)). A slight increase in the OD was observed for the highest concentration indicating a slight increase in OD due to the presence of NPs in the assay.

To detect the potential binding of Au-NPs to antibodies (see Figure S10: NP in medium (as sample)) NPs are spiked in instead of the antigen. Therefore Au-NPs are diluted in media, washed according to protocol and finally the substrate was applied. No changes in OD were observed. This indicates that Au-NPs do not bind to the antibodies.

Finally, the binding capability of Au-NPs to the antigen was assessed (see Figure 10S: NP + 500 pg/ml Standard (as sample)) by spiking in the NPs together with the antigen. Different concentrations of Au-NP were diluted in 500 pg/ml TNF-α, processed according to the protocol and in the end the substrate was applied. A slight increase in OD was observed for Au-NP I and III starting at a concentration of 50 µg/ml. This however, was not detected for Au-NP II. This indicates that these two Au-NPs might be able to bind to the antigen, leading to an amplification of the signal and thereby producing false positive results in the cellular assay. However, one has to consider the observed increase in “intrinsic” OD of the particles alone which might account for part of this increase. In the spike-in approach described here it is assumed that all ENMs applied to the cells end up in the ELISA analysis. This is a "worst-case scenario" and not very likely to occur. This is supported by the observation that the cellular assay revealed no positive result for any of the Au-NPs at any concentration. Therefore these minor interferences are scientifically interesting, but negligible regarding the results obtained in the cellular ELISA assays.

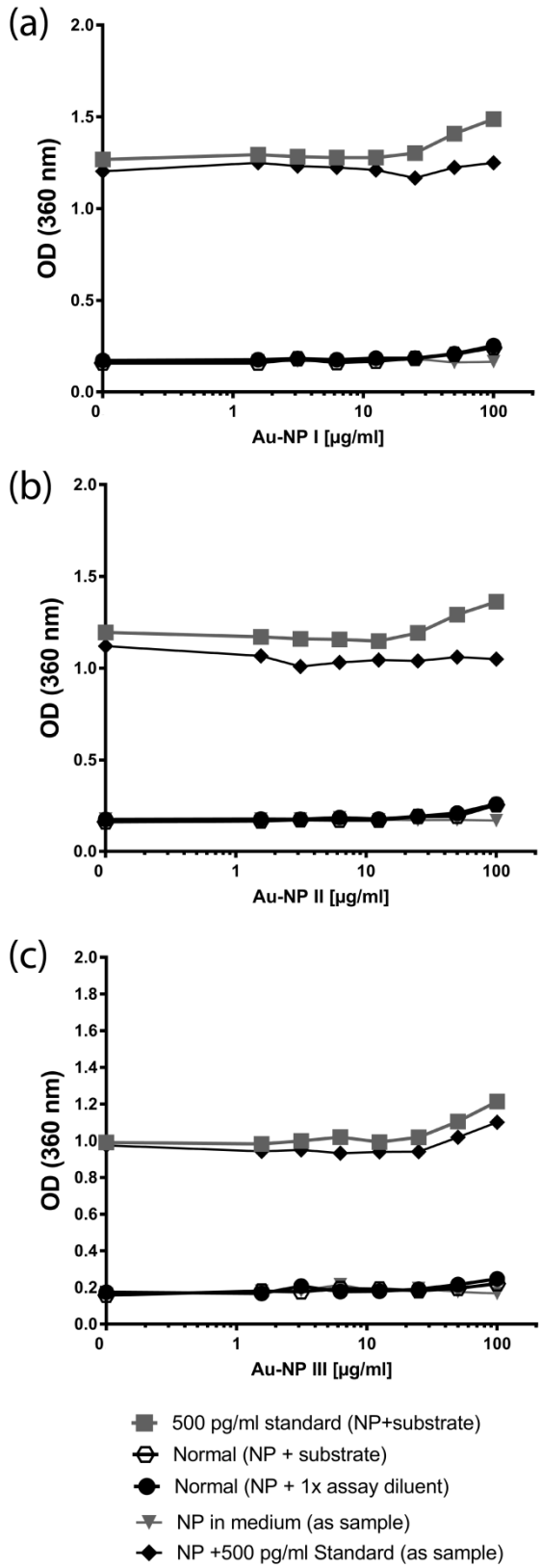

Figure S10. Au-NP interference with the ELISA for TNF-α detection. Absorbance values of Au-NP I (a), Au-NP II (b) and Au-NP III (c) were assessed for four different parameters in a cell free setup. Potential intrinsic catalytic activity of Au-NPs was assessed in the presence and absence of the antigen TNF-α. As in both cases the OD increases at high concentrations a

certain intrinsic catalytic activity of the Au-NPs is expected. A slight increase in the OD is caused by the presence of Au-NPs when prepared in assay diluent without application of antigen or substrate. Spiking in Au-NPs instead of the antigen to assess the potential binding of NPs to antibodies reveals no changes in OD. The binding capability of Au-NPs to the antigen was assessed by spiking in the NPs together with the antigen and a slight increase in OD is observed for Au-NP I and III starting at a concentration of 50 µg/ml. Data shown represent the mean of one to two independent experiments.

References

1. L. Belyanskaya, P. Manser, P. Spohn, A. Bruinink and P. Wick, *Carbon*, 2007, **45**, 2643-2648.
2. A. Casey, E. Herzog, M. Davoren, F. M. Lyng, H. J. Byrne and G. Chambers, *Carbon*, 2007, **45**, 1425-1432.
3. L. Guo, A. Von Dem Bussche, M. Buechner, A. H. Yan, A. B. Kane and R. H. Hurt, *Small*, 2008, **4**, 721-727.
4. C. Hirsch, M. Roesslein, H. F. Krug and P. Wick, *Nanomedicine (Lond)*, 2011, **6**, 837-847.
5. C. Hirsch, J. P. Kaiser, F. Wessling, K. Fischer, M. Roesslein, P. Wick and H. F. Krug, *Journal of Physics: Conference Series*, 2011, **304**, 012053.
6. N. A. Monteiro-Riviere and A. O. Inman, *Carbon*, 2006, **44**, 1070-1078.
7. A. Kroll, M. H. Pillukat, D. Hahn and J. Schnekenburger, *European Journal of Pharmaceutics and Biopharmaceutics*, 2009, **72**, 370-377.
8. A. Bachmatiuk, R. G. Mendes, C. Hirsch, C. Jahne, M. R. Lohe, J. Grothe, S. Kaskel, L. Fu, R. Klingeler, J. Eckert, P. Wick and M. H. Rummeli, *Acs Nano*, 2013, **7**, 10552-10562.
9. h. w. n. i. DaNa, https://www.nanopartikel.info/).